American Journal of Pathology, Vol. 165, No. 4, October 2004

Review

Proteomics in Diagnostic Pathology

Profiling and Imaging Proteins Directly in Tissue Sections

Pierre Chaurand,*† Melinda E. Sanders,‡ Roy A. Jensen,‡ and Richard M. Caprioli*†

From the Mass Spectrometry Research Center, the Department of Biochemistry,† and the Department of Pathology,‡ Vanderbilt University, Nashville, Tennessee*

Direct tissue profiling and imaging mass spectrometry (MS) provide a molecular assessment of numerous expressed proteins within a tissue sample. MALDI MS (matrix-assisted laser desorption ionization) analysis of thin tissue sections results in the visualization of 500 to 1000 individual protein signals in the molecular weight range from 2000 to over 200,000. These signals directly correlate with protein distribution within a specific region of the tissue sample. The systematic investigation of the section allows the construction of ion density maps, or specific molecular images, for virtually every signal detected in the analysis. Ultimately, hundreds of images, each at a specific molecular weight, may be obtained. To date, profiling and imaging MS has been applied to multiple diseased tissues, including human non-small cell lung tumors, gliomas, and breast tumors. Interrogation of the resulting complex MS data sets using modern biocomputational tools has resulted in identification of both disease-state and patient-prognosis specific protein patterns. These studies suggest that such proteomic information will become more and more important in assessing disease progression, prognosis, and drug efficacy. Molecular histology has been known for some time and its value clear in the field of pathology. Imaging mass spectrometry brings a new dimension of molecular data, one focusing on the disease phenotype. The present article reviews the state of the art of the technology and its complementarity with traditional histopathological analyses. ***(Am J Pathol 2004, 165:1057–1068)***

Advances in molecular biology and molecular technologies over recent years will have a profound impact on diagnostic pathology in the years to come. Molecular information derived from genomics and proteomics will be of critical importance to our understanding of molecular pathogenesis, improving therapeutic efficacy, and enhancing the quality of information that is provided to clinicians so as to markedly improve patient outcomes. Indeed, one can anticipate that these revolutionary advances will be an important complement to traditional methods of histopathological analysis in the future. It is believed that these new approaches will significantly impact three major areas: tissue-based diagnosis, prognosis determination, and prediction of response to specific modes of therapy. In addition, the identification of molecular signatures that are necessary precursors to disease or are early markers of disease should provide reliable methods of early detection for a broad spectrum of disease processes.

The development of modern medicine had its basis in diagnostic pathology in the mid-nineteenth century. As specific patterns of disease were recognized and their etiologies investigated, it became clear that recognition of these, and understanding their pathogenesis, would be the primary process for developing appropriate therapies for the vast majority of disorders that afflicted the human condition. Since then, the discipline of pathology has played a vital role in establishing not only the tissue diagnosis but also the prognosis of particular diseases based on specific pathological findings. Objective prognostication is critical in predicting which forms of therapy might be most effective. While routine diagnostic pathology represents the gold standard and plays an integral role in evaluating prognosis and predicting the response to therapy for groups of patients with a specific disease type, the application of these techniques often falls short in evaluating individual patients.

The addition of molecular techniques to our armamentarium for cancer has and will continue to increase our

Supported by National Institutes of Health grant GM 58008–05 and National Cancer Institute grant CA 86243–02 (P.C. and R.M.C.).

Accepted for publication July 15, 2004.

Address reprint requests to Richard Caprioli, Mass Spectrometry Research Center, 9160 MRB III, Vanderbilt University, Nashville TN, 37232-8575. E-mail: r.caprioli@vanderbilt.edu.

predictive and prognostic power, enabling more accurate classification of tumors and individual tailoring of cancer therapy. Ideally, molecular evaluation would be performed on an ongoing basis such that at any particular point the therapeutic susceptibilities of the predominant subclone within a tumor could be identified and appropriate therapy could be administered. Later, as resistant subclones emerge, the patient could be given alternative treatments selected for their efficacy against a new set of markers. In this approach, cancer would be viewed as a chronic disease requiring continual monitoring to maintain a therapeutic edge over emergent clones.

It is not yet clear how soon and to what extent these molecular phenotyping techniques will be integrated into surgical pathology. Indeed, one must take care to introduce those protocols that add value and not eliminate those that are established with proven value. For example, for solid tumors the current protocols in pathology will continue to be effective as long as surgical therapy continues to be the primary and most effective form of treatment. With rare exceptions, surgical extirpation of cancer before its metastatic spread provides the best chance of cure. Local control often represents an important aspect of achieving this end. Routine histopathological determination of margin status has consistently been shown to be an excellent predictor of the presence or absence of residual disease, and therefore, the likelihood of local recurrence. While there have been some attempts to examine margin status via molecular methods, no currently available molecular method demonstrates sufficient specificity or sensitivity to challenge the supremacy of surgical pathology. Nevertheless, it is clear that molecular methods will bring new insights and new approaches, which will require validation with current protocols.

Although both genomics and proteomics provide such molecular signatures each in their own way, this article will focus on proteomics in terms of its potential to integrate a detailed molecular phenotype of disease into diagnostic pathology protocols. Since the sum of the temporal alterations in proteins ultimately promotes or reflects the particular disease state, proteins represent an array of potential tumor specific markers and drug targets. The examination of global protein expression required in understanding the inter-relatedness of multiple gene transduction pathways in disease is now possible.

Protein Analysis Using Mass Spectrometry

In recent years, mass spectrometry (MS) has become an indispensable tool for proteomic studies, that is, the detection, identification, and characterization of the protein component of cells, tissues, and organs at any time point in both health and disease.[1–7] For protein analysis, several different types of instruments and protocols allow for the determination of molecular weight, primary and higher order structure, post-translational modifications, quantitation, and localization. Desorption and ionization techniques such as matrix-assisted laser desorption ionization mass spectrometry (MALDI MS)[8,9] and significant improvements of time-of-flight mass spectrometers[10,11] have literally revolutionized our ability to analyze proteins. These improvements offer levels of sensitivity and mass accuracy never before achieved for the detection, identification, and structural characterization of proteins. It is now possible to routinely measure molecular weights above 200 kDa as well as obtain low parts per million mass measurement accuracy for the determination of peptides and proteins. Protein identification has been greatly facilitated because of the rapid expansion of protein and gene databases. Modern mass spectrometers can now rapidly map and fragment peptides that result from protease digestion to identify proteins and obtain sequence information.

MALDI MS is particularly useful in this regard because of its potential for high throughput and ability to provide information on the localization of molecules in a sample. Recent application of this technology to the analysis of thin tissue sections clearly shows retention of spatial and anatomical relationships permitting the complex interaction between diseased cells and their environment to be studied at the molecular level.[12–18] From the systematic analysis of a single tissue section, protein-specific maps directly correlated with tissue architecture may be simultaneously obtained for over a thousand different protein species.[12] The potential for this type of analysis in which the spatial distribution of specific molecular species can be mapped throughout a tissue section is particularly exciting for the study of disease.[19–21] While this capability is routinely available for known individual proteins via immunohistochemistry, imaging mass spectrometry (IMS) offers the potential for the simultaneous analysis of many molecular species present in a single tumor regardless of the availability of specific antibodies or knowledge of the identity of the specific protein. In addition, this technology also permits imaging tissue distribution of low molecular weight compounds, such as drugs and metabolites,[22,23] opening new possibilities for the measurement of concomitant protein changes in specific tissues after systemic drug administration. Finally, when coupled with laser capture microdissection (LCM),[24–26] MALDI MS is capable of analyzing many proteins from as few as 10 to 50 cells without any requirement to amplify the material.[17,27–29] In combination with rapid advances in informatics, MS offers the capacity for an entirely new and highly precise means of analyzing disease tissue. For example, with continued advances in instrumentation and the understanding of molecular pathogenesis, it should be possible to determine the proteomic profile of a tumor within the time frame currently used for intraoperative frozen section examination. This information could significantly impact the course of therapy for a particular tumor and would be available before the patient leaves the operating room.

In the following paragraphs, three aspects of MS technology are addressed: 1) details of the profiling and imaging MS technology and how it is used for tissue section analyses; 2) specific applications to diagnosis and prognosis of disease as well as its usefulness in

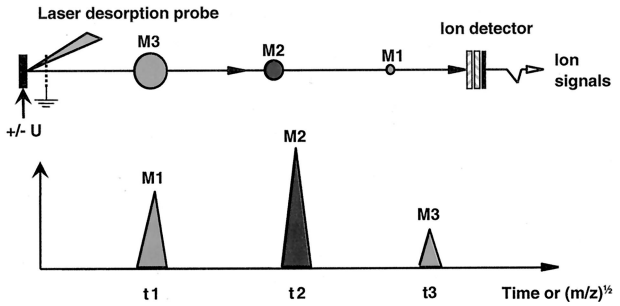

Figure 1. Principle of time-of-flight mass spectrometry. Ions formed by laser irradiation in the source area are accelerated by a positive (or negative) potential difference applied between the sample plate and the extracting electrode(s). Ions of the same nominal charge acquire the same kinetic energy; however, their respective velocities will depend on their mass. Ions are then separated in time based on their velocities in a field free time-of-flight tube and are finally detected by an ion detector. The time each ion takes to travel through the mass spectrometer is precisely measured. After instrument calibration, the ion flight times are converted to mass. Effectively, time-of-flight mass spectrometers measure the mass-to-charge (m/z) ratios of ions.

predicting response to therapy; and 3) perspectives on future developments in association with pathology.

Profiling and Imaging Tissues by Mass Spectrometry

Imaging mass spectrometry is a relatively new technology that takes advantage of the methodology and instrumentation of MALDI mass spectrometry.[13–15,18] Briefly, molecules are desorbed from a sample that has been coated with an energy absorbing matrix, the latter being a low molecular weight organic crystalline compound. In the desorption process, molecules become protonated and typically carry one positive charge. These desorbed ions are accelerated by a high voltage grid and traverse a flight tube striking a detector at the end of this tube. Since the acceleration energy is the same for all ions, the laws of conservation of energy dictate that small ions will traverse the flight tube faster relative to larger ions. Thus, the time of flight of the ions is proportional to mass. Figure 1 describes the principle of time-of-flight mass spectrometry. The analyses discussed here were performed at +25 kV of accelerating potential on Applied Biosystems, Inc. (Framingham, MA) time-of-flight mass spectrometers under optimized delayed extraction conditions (focusing at mass-to-charge (m/z) ~15,000 allowing for optimum resolution throughout the studied mass range) using a 337 nm N_2 laser capable of operating at repetition rates of 3 or 20 Hz. The laser spot on the target, representing a pixel of the final image, is roughly circular with a 50-μm diameter. Ion image acquisition was performed by custom software,[16,30] that interfaces with the instrument controller and acquisition software. The software controls data acquisition over a predetermined area and reconstructs ion density maps or images by plotting measured signal intensities over the area analyzed. If desired, such molecular weight-specific images can be produced for every molecular signal acquired.

Protein profiles and images can be obtained directly from thin tissue sections cut on a cryostat from fresh-frozen tissue blocks (Figure 2). Tissue biopsies or other relevant tissue samples should be frozen immediately after acquisition in liquid nitrogen or isopentane to preserve the sample's morphology and minimize protein degradation through enzymatic proteolysis. For most applications, 5- to 20-μm thick sections are cut at −15°C (exact cutting temperature is tissue dependent) and thaw-mounted on an electrically conductive sample plate. The sections are dried in a dessicator for several minutes before MALDI matrix deposition. The MALDI matrix can either be deposited as individual droplets (spotted) or as a homogeneous layer (coated) on the tissue section, depending on the spatial resolution required for the analysis (Figure 2).

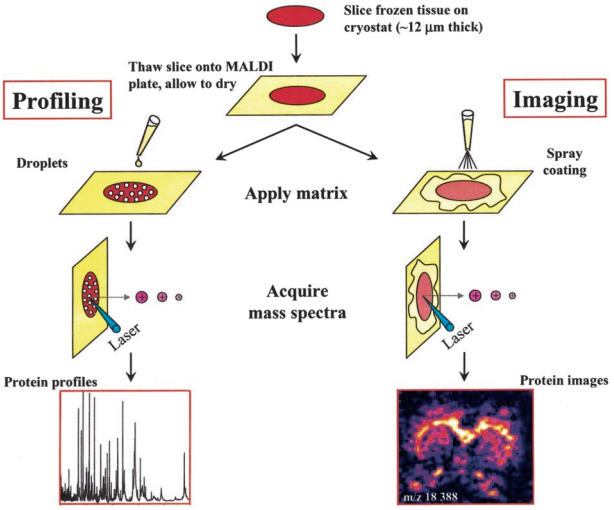

Figure 2. Scheme outlining the different steps involved for profiling and imaging mass spectrometry of mammalian tissue samples. See text for details (from reference[18]).

Generally, sinapinic acid is an excellent matrix for the analysis of proteins,[31] although α-cyano-4-hydroxycinamic acid may also be used for the profiling of peptides and lower molecular weight proteins.[32,33] Small volumes of matrix (typically 200 to 500 nL) can be directly spotted onto a tissue section using an automatic pipette (Figure 2). Smaller drop sizes (5 to 50 nL) can be applied with a fine capillary attached to a Hamilton-type syringe containing the matrix. In this case, matrix deposition is performed under low to medium magnification to precisely deposit the matrix droplets at the desired tissue coordinates. The resulting matrix spots have a crystal density that covers about 50% of the area with individual crystals being about 20 to 200 μm in length. On analysis (Figure 2), the resulting mass spectra typically yield 300 to 1000 signals, of various intensities over an intensity range of three orders of magnitude and in a m/z range from m/z 2000 up to, and in some cases over, m/z 200,000.[14] However, because of the inability of time-of-flight mass analyzers to resolve[34] and efficiently detect higher molecular weight compounds,[35,36] most of the signals detected are below m/z 50,000. In this mass range, signal resolution (full width at half-maximum definition) spends from about 1000 for the focused ions to about 100 for the higher molecular weight ions. In general, the most intense

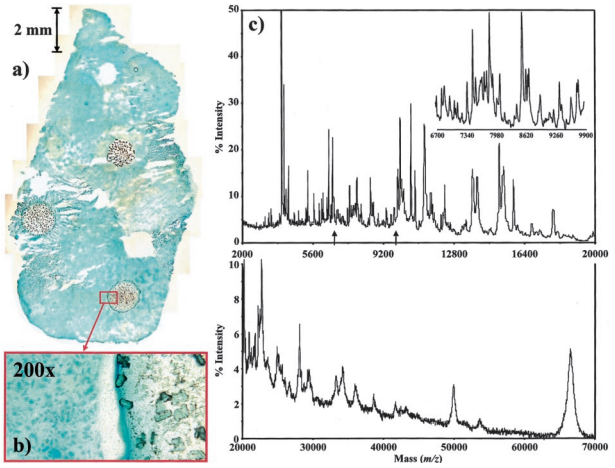

Figure 3. Analysis a 12-μm methylene blue-stained human grade IV glioma section. **a:** Photomicrograph of the section. Several matrix droplets are visible on the surface of the section. The **inset b:** details the edge of a droplet where numerous matrix crystals are visible. **c:** MALDI MS protein profile acquired from the lower droplet. The **inset** details the *m/z* range from 6700 to 9900 (**arrows**).

signals come from the most abundant protein species. The exact sensitivity of the technology is however hard to estimate because exact amounts of proteins within a specific tissue are generally not well known. The profiles recovered have been found to be extremely specific to a given tissue type and, when analyzing serial sections, very reproducible. Reproducibility was also observed when analyzing sections of the same tissue but sampled in different animals or individuals.

One of the latest tissue analysis protocols developed utilizes optically transparent glass slides as target plates (which have a thin conductive coating on the surface) together with MALDI MS friendly tissue staining protocols.[37] This makes possible the microscopic evaluation of a tissue section by a pathologist followed by the molecular imaging of the same section by MS. Figure 3 presents the analysis of a grade IV human glioma section after staining with methylene blue, which provides strong nuclear as well as faint cytoplasmic staining. MALDI MS analysis was performed on a highly cellular region of the tumor. The resulting spectrum displays signals in the *m/z* range from 2000 to 70,000.

In the imaging experiment, an important aspect of sample preparation methods is the homogeneous deposition of the MALDI matrix on the sample in such a way as to avoid significant lateral migration of proteins on the surface of the section (Figure 2). There are several methods for applying matrix to tissue sections, eg, addition of individual droplets, and spraying by nebulization, acoustic waves, and electrospray deposition. Although each method has its own advantages and drawbacks, the following protocol is generally suitable for most tissues. Fixing of tissues must be done (if at all) using reagents and solvents that do not react with or cross-link proteins. Sections mounted on the target plate are dehydrated with a two-step ethanol-based protocol: 15 seconds in 70% ethanol and 15 seconds in 100% ethanol. After complete evaporation of the ethanol (a few minutes in a dessicator), the sections are coated with matrix solution using a pneumatic hand-held Venturi glass sprayer. At this stage, special care needs to be taken not to over-wet the section. On average, 10 spray cycles are necessary to achieve a thin, relatively homogeneous matrix coating that covers the entire tissue section. The coating procedure may be monitored under a microscope to assess crystal size and density.[31] In terms of the MS instrument setup, instrument control software is used to set a data acquisition grid that defines a discrete Cartesian pattern across the sample surface.[16,30,38,39] This pattern has a fixed center to center distance between spots, typically 50 to 150 μm depending on the dimensions of the section and the imaging resolution required. The mass spectrometric data are then acquired using this grid pattern with a predetermined number of laser shots per grid coordinate. Data processing (image reconstruction) is done with specialized software[16,30,38,39] by integrating signal intensities at desired *m/z* values across the data set (Figure 2). The time required for data acquisition depends on the area of the tissue to be analyzed and the resolution (number of pixels) required. Acquisition of high-resolution images may require several tens of thousands of individual spectra and can generate large data files (1 to 2 gigabytes). An imaging experiment becomes necessary when high-resolution protein distribution information within a tissue section is of importance. For example, when analyzing tumor biopsies, analysis of the precise architectural arrangement of the various cell types present in the section and the differentially expressed MS signals may lead to a better understanding of molecular interactions between a tumor and its surrounding stroma. High-resolution images are also desirable when there is defined substructure present. Although the local protein composition may affect the ionization and therefore, detection of a monitored protein species (ion suppression effects), good agreements are generally observed between images obtained by IMS and other protein imaging techniques such as immunohistochemistry.[17]

Presented in Figure 4 is the analysis of a mouse coronal brain section by imaging mass spectrometry.[18] Figure 4a presents a photomicrograph of a 12-μm section (Bregma +0.74 mm) mounted on a glass slide and stained with hematoxylin and eosin (H&E). Substructures such as the cerebral cortex, the corpus callosum, and the striatum are clearly visible (labeled 1, 2, and 3 on Figure 4a) and have been highlighted on the right side of the section. The next serial section was imaged by MS with a resolution of 50 μm, analyzing a 142 $\times$ 199 data point grid (representing 28,258 mass spectra). Each spectrum is the result of the average of 40 laser shots. A signal threshold was applied to remove background noise from each individual spectrum. Figure 4b presents a survey protein profile obtained from the section after matrix deposition, averaging all of the mass spectra acquired from the area of the section. From this profile, hundreds of distinct mass signals, some with very low signal intensities, were observed in the *m/z* range from 2000 to 35,000. The complexity of the data is well illustrated in the inset of Figure 4b, displaying the profile in the *m/z* range from 8000 to 10,500 where over 50 distinct mass signals were

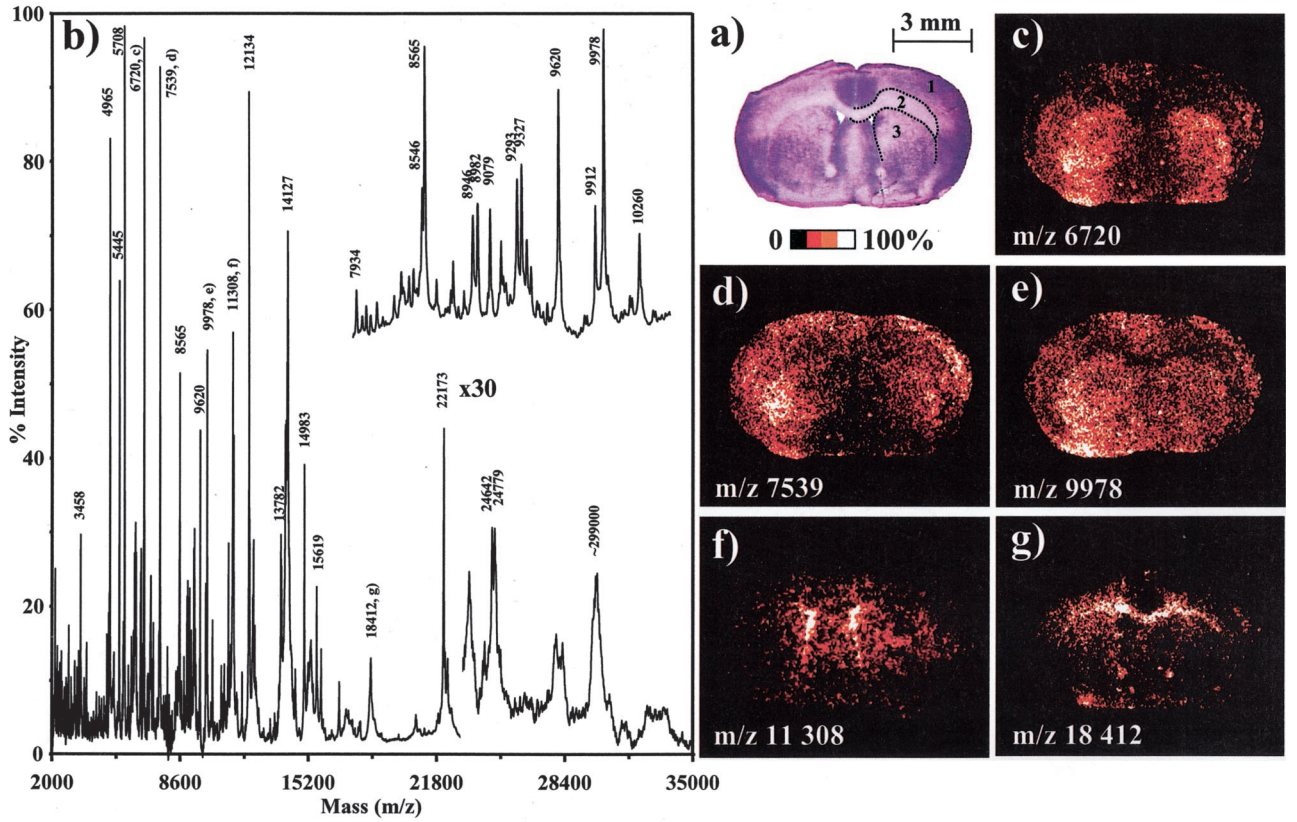

Figure 4. IMS analysis of a 12-μm coronal mouse brain section (adapted from reference[18]). **a:** Photomicrograph of an H&E-stained section showing different anatomical brain substructures: 1, cerebral cortex; 2, corpus callosum; 3, striatum. **b:** Survey protein profile obtained after homogeneous matrix deposition from a subsequent serial section. **c–g:** Ion density maps obtained at different *m/z* values with an imaging resolution of 50 μm. The ion density maps are depicted as pseudo-color images with **white** representing the highest protein concentration and **black** the lowest.

detected. Figure 4, c to g, presents five ion density maps obtained for different protein signals detected in the survey scan (see signals c to g in Figure 4b). Certain signals were found expressed in very specific regions of the section. For example the signal at *m/z* 18,412 is almost uniquely found in the corpus callosum, while the signal at *m/z* 6720 is most abundant in the striatum. A second example of a molecular image produced in this way is given in Figure 5, obtained from a section of rat kidney. Twelve-μm sections were cut and mounted on the target surface. In this case, matrix was deposited after section dehydration using an automated spotter, generating a Cartesian small droplet array over the surface of the section.[40,41] Data acquisition was performed at 20 Hz averaging signals from 400 laser shots per droplet. Droplets were deposited every 250 μm on the section and 1518 individual spectra were recorded. Figure 5a presents a portion of the survey scan in the *m/z* range from 9850 to 10,050. Two high intensity signals that are close in molecular weight at *m/z* 9943 and 9979, respectively, were observed. The corresponding ion images for those two proteins are presented in Figure 5, b to d, showing different distributions throughout the section, one expressed predominantly in the medulla and the other in the cortex.

Laser capture microdissection (LCM) is a newly developed technology that permits the isolation of single cells or single populations of cells from thin tissue sections (typically 5 to 10 μm in thickness) mounted on a glass slide.[24–26] In combination with MS, this promises to help acquire protein signatures from a single cell type within a heterogeneous sample. In one common type of LCM technology, a narrow laser beam (7.5 to 30 μm in diameter) is fired at a heat-sensitive transparent polymer film on a cap that is in contact with the tissue. When the

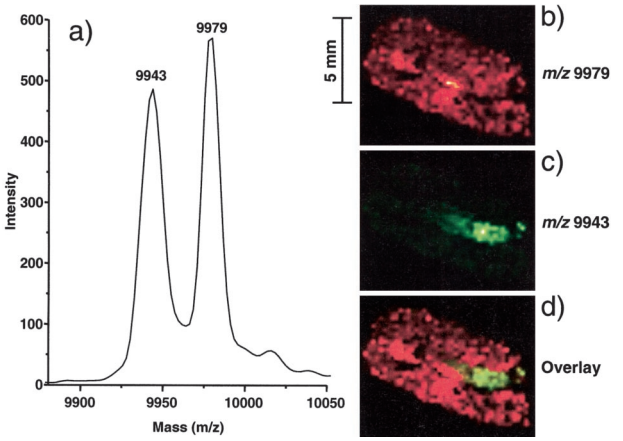

Figure 5. IMS analysis of a 12-μm rat kidney section. **a:** Partial survey protein profile in the *m/z* range from 9850 to 10,050, obtained after homogeneous matrix deposition on the section, showing two strong signals at *m/z* 9943 and *m/z* 9979. **b–d:** Ion density maps obtained for *m/z* 9943 and *m/z* 9979 with an imaging resolution of 250 μm.

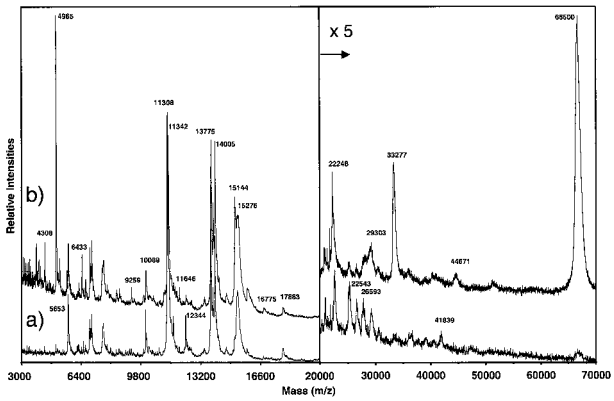

Figure 6. MALDI MS protein profiles obtained from epithelial cells (lobular units and ducts) (**a**) and stroma cells (**b**), sampled by laser capture microdissection from human breast tissue.

polymer is heated, it adheres to the cell(s) of interest and these cells are subsequently removed from the section when the cap is lifted. In the examples given in this article, cells were microdissected using the PixCell II LCM System (Arcturus Inc., Mountain View, CA). The membrane containing the captured cells is then mounted on the target plate of the MS using conductive double-sided tape. The cells are spotted with small volumes of matrix (sinapinic acid, prepared as mentioned above) using a thin capillary and analyzed.[28] Although protein profiles have been obtained from cells microdissected from paraffin-embedded[27] and frozen archived tissues,[29] best results are obtained from cells dissected from fresh-frozen tissue sections.[17,28] Figure 6 shows two proteins profiles obtained from microdissected mammary epithelium (lobular units and ducts) and mammary stroma from a reduction mammoplasty specimen. Numerous signals were found to be differentially expressed between these two cell populations.

Diagnostic and Prognostic Assessments of Cancer

The first published study using mass spectrometry to subclassify tumors and predict clinical outcome was recently reported.[19] MALDI TOF MS was used to generate protein spectra directly from frozen tissue sections from 79 surgically resected lung tumors and 14 normal lung specimens.[19] For optical evaluation and comparison, serial sections were stained with hematoxylin and eosin (H&E) and examined by a board-certified pathologist. MALDI MS data were collected using standardized instrumental acquisition parameters and processing parameters including calibration, baseline correction, and smoothing. Before statistical analysis, common protein signals across multiple samples were aligned to create mass (*m/z*) windows that maximize the number of peaks in a bin across the sample set and minimize the number of peaks in a bin from the same sample. These bins were used to define individual protein peaks within a large data set for statistical analysis.

The full statistical analysis has been detailed elsewhere.[19] Briefly, the proteomic spectra were analyzed using unsupervised and supervised hierarchical multivariant cluster analyses to subclassify the samples according to their expression patterns and to look for relationships between tumor subtypes and clinical outcome. A class prediction model was created using the protein profiles from a training cohort of 34 primary lung tumors, two pulmonary metastases of previously resected non-small cell lung carcinomas (NSCLC), one pulmonary carcinoid, five metastases to the lung from other sites, and eight normal lung samples. From among more than 1600 individual protein signals detected across all patient samples, 82 signals differentially expressed between lung tumors and normal lung were selected as discriminators (Table 1). When this model was applied to a blinded test cohort of 32 primary NSCLC, five metastases to the lung, and six normal lung samples to estimate the rate of misclassification, their proteomic patterns correctly classified all samples as either tumor or normal (Table 1).

Using similar class prediction models, it was demonstrated that primary NSCLC could be distinguished from normal lung based on 91 MS signals with 100% accuracy (Table 1). Representative examples of MALDI MS spectra from three different tissue samples from this study (two primary NSCLC and one normal lung tissue) are presented in Figure 7a. Examples of MS peaks which were identified by the statistical analysis as optimum discriminators between the histological groups are indicated by asterisks. Figure 7b shows the hierarchical cluster analysis of the 34 lung tumors and eight normal lung tissues in the training cohort according to the protein expression patterns of these 91 MS signals. Next, they found that 27 MS signals could discriminate between the major histological subtypes of NSCLC: adenocarcinoma, squamous cell carcinoma, and large cell with near perfect accuracy. Figure 7c presents the classification obtained for the training data set consisting of the protein expression

Table 1. Classification of Samples in Training and Test Cohort According to the Protein Expression Profiles Measured by MALDI MS Directly from Normal and NSCLC Tissue Sections (adapted from reference[19])

Samples (training, test)	No. of differentially expressed peaks	No. of misclassified samples (% correct)
Normal lung versus lung tumor (8,6) (42,37)	82	0, 0 (100)
Normal lung versus primary NSCLC (8, 6) (34,32)	91	0, 0 (100)
Adenocarcinoma versus squamous-cell (14, 13) (15, 16)	20	0, 0 (100)
Adenocarcinoma versus large-cell (14, 13) (5, 3)	20	0, 1 (100, 94)
Squamous-cell versus large-cell (15, 16) (5, 3)	12	0, 0 (100)
Nodal metastasis negative versus positive (20, 25) (14, 7)	2	5, 8 (85, 75)

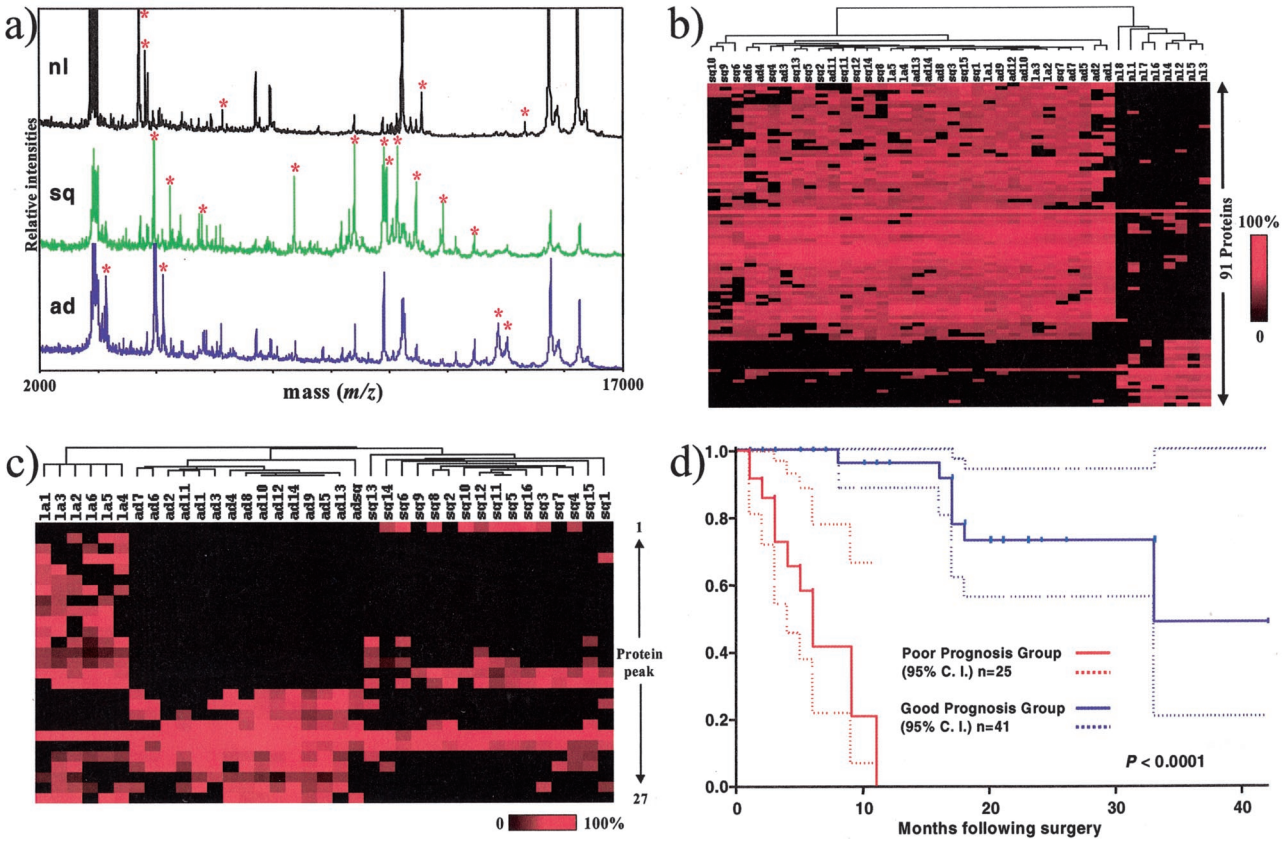

Figure 7. Analysis of proteomic patterns in non-small cell lung cancer (adapted from reference[19]). **a:** MALDI MS protein profiles obtained from normal and cancerous human lung tissue sections. **b:** Hierarchical cluster analysis of eight normal lung tissue and 34 resected primary NSCLC samples according to the protein expression patterns of 91 protein signals. Each **row** represents an individual protein signal and each **column** represents an individual sample. The protein signals allow differentiation with 100% accuracy between normal tissue and NSCLC samples. **c:** Hierarchical cluster analysis of 37 resected primary NSCLC samples according to the protein expression patterns of 27 protein signals. The protein signals allow differentiation with 100% accuracy between the different types of NSCLC. (nl), normal; (sq), squamous cell carcinoma; (ad), adenocarcinoma; (la), large cell carcinoma. **d:** Kaplan-Meier survival curves for groups with poor and good prognosis according to proteomic pattern comprised of 15 distinct MS peaks.

profiles of NSCLC. The NSCLC were perfectly separated into known major histological groups: adenocarcinoma (n = 14), squamous cell carcinoma (n = 15), and large cell carcinoma (n = 5). These models were then applied to the blinded validation samples in the test cohort to define the misclassification rate. The results from these analyses are also presented in Table 1. Only one large cell carcinoma was misclassified as an adenocarcinoma. The authors suggest, however, that this tumor may have been an adenocarcinoma that was too poorly differentiated to be identified as such by light microscopy. Similar class prediction models were also able to distinguish primary lung tumors from tumors metastatic to the lung, a finding that has the potential to directly impact clinical care decisions.

The class prediction models based on differentially expressed peaks were also able to predict nodal involvement. The proteomic patterns in primary NSCLC associated with the nodal status as discovered at the time of lymph node dissection during the primary tumor resection, allowed grouping of the samples as either node negative or pathologically node positive.[19] Nodal involvement was determined by light microscopy of resected nodes with no staining or PCR amplification classically used to detect occult metastases. According to the statistical criteria used, two protein markers were related to mediastinal nodal involvement. Using the expression patterns of these discriminatory proteins, 29 out of 34 tumors (85% accuracy) were correctly classified (see Table 1). This classification was then applied to the blinded test cohort and correctly classified 24 out of 32 tumors (75% accuracy). Although there were several apparently misclassified samples, the possibility of unsampled or undersampled nodes can not be entirely excluded. The accuracy of the proteomic pattern is, in fact, comparable to standard staging techniques and better than any other molecular markers identified to date. Since nodal involvement is one of the most important factors used to determine therapeutic options, confirmation of this molecular approach by investigating a larger sample set may prove to be extremely useful for future use in a clinical setting.

The study described above sought to identify proteomic pattern in lung cancer independent of histology, currently the gold standard for prognostic assessment, which would be predictive of patient outcome.[19] They statistically analyzed the protein expression profiles of 66 primary NSCLC for expression patterns correlated with survival. They found 15 distinct mass peaks which could segregate the NSCLC patients into a group with poor prognosis (median survival, 6 months; n = 25) and one

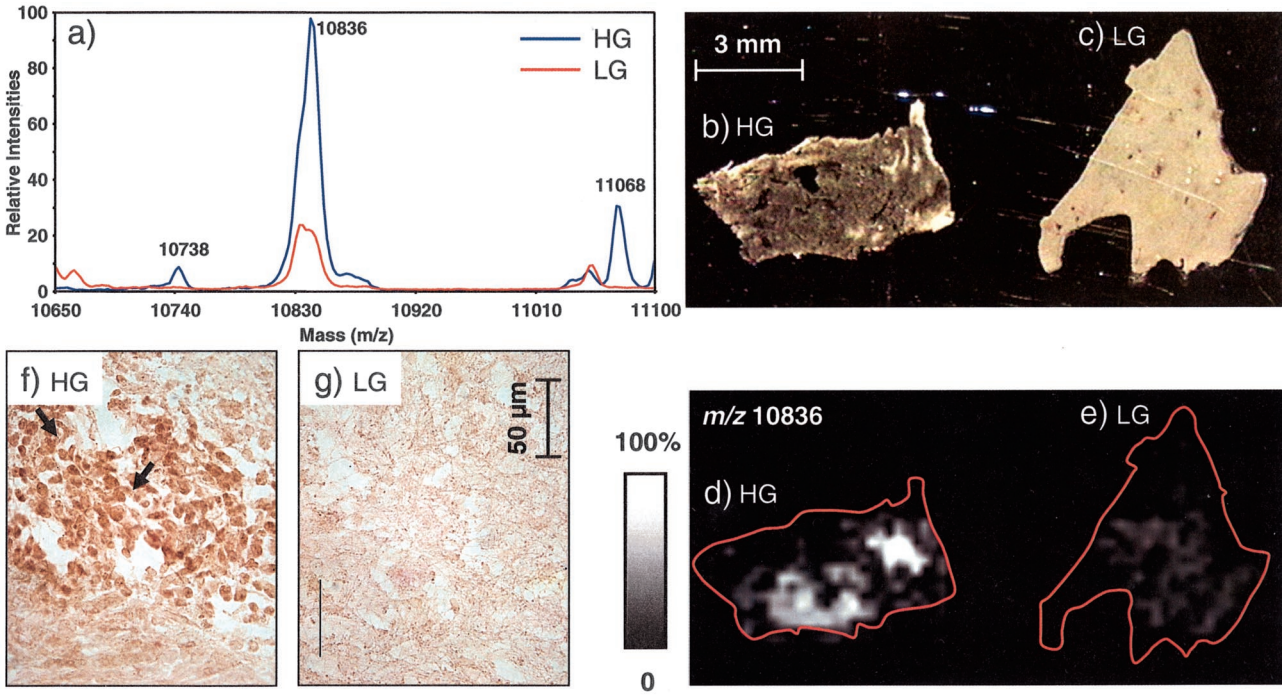

Figure 8. Localization of the S100B protein in human low-grade and high-grade glioma biopsies by imaging mass spectrometry and immunohistochemistry. **a:** Partial survey MALDI MS protein profiles obtained from low-grade (LG, **orange trace**) and high-grade (HG, **blue trace**) 12-μm glioma sections. The signal at *m/z* 10836 was identified as the S100B protein. Photomicrographs of high-grade (**b**) and low-grade (**c**) 12-μm glioma sections. S100B ion intensity maps obtained from high-grade (**d**) and low-grade (**e**) glioma sections. High magnification photomicrographs obtained from high-grade (**f**) and low-grade (**g**) glioma sections after immunostaining for the S100B protein.

with good prognosis (median survival, 33 months; n = 41). Figure 7d presents the corresponding Kaplan-Meier survival curves for these groups according to the protein expression patterns of these 15 mass peaks. Even after adjustment for tumor size, nodal status, stage, and tumor grade, this strong association was also demonstrated using an independent multivariate Cox proportional hazards model. If these observations can be confirmed in larger studies, the prognostic power of this 15-peak profile would exceed that of almost any previously reported molecular markers.

Preliminary results of similar studies of human glioma biopsies has also been reported that demonstrate that proteomic patterns can be used to distinguish glioma tissue from normal brain tissue as well as subclassify gliomas by histological grade.[20] In this study, 20 prospectively collected, snap-frozen normal brain and brain tumor specimens were examined using MALDI MS. Peptide and protein expression were compared and the patterns assessed through hierarchical cluster analysis. The mass spectral patterns could reliably distinguish gliomas from non-tumor brain tissue as well as subclassify grade IV gliomas from grades II and III. The mass signals found to statistically discriminate between normal and tumor and the different grades of cancer are currently being identified. Biomarker identification is performed by well-established methods that consist of extraction of the proteins from the tissue followed by protein separation (RP-HPLC and size exclusion). After screening by MALDI MS, the HPLC fractions containing the targeted molecular weight markers are digested with trypsin and the resulting peptides mapped and sequenced by mass spectrometry. The proteins are identified by interrogating gene or protein databases with the experimentally recovered sequences.[12,17,42] Figure 8 presents the simultaneous analysis by imaging mass spectrometry of two 12-μm sections obtained from grade II (low-grade) and grade IV (high-grade) resected human glioma biopsies. The sections were coated with matrix using the automated spotter, and the images were acquired with a lateral resolution of 250 μm. Figure 8a presents partial survey protein profiles obtained from the low-grade (orange trace) and high-grade glioma (blue trace). In the *m/z* range displayed, several signals were expressed with higher intensities in the high-grade biopsy. In particular, a signal at *m/z* 10,836, identified as S100β protein (Swiss-Prot Accession Number P04271), was found increased by about a factor of four in the high-grade sample. Figure 8, b to e, presents the photomicrographs for the high-grade and low-grade sections (Figure 8, b and c, respectively) before matrix deposition, and the corresponding mass spectrometric ion density maps (Figure 8, d and e, respectively) obtained when integrating the signal for the S100β protein at *m/z* 10,836. The images clearly show stronger S100β protein expression in the high-grade tumor with respect to the low-grade tumor. In parallel, S100β protein expression levels between low-grade and high-grade gliomas were also investigated by immunohistochemistry. Figure 8, f and g, displays magnified photomicrographs of high-grade and low-grade glioma tissue sections (cut from the same biopsies investigated by IMS) after immunoreaction (epifluorescence

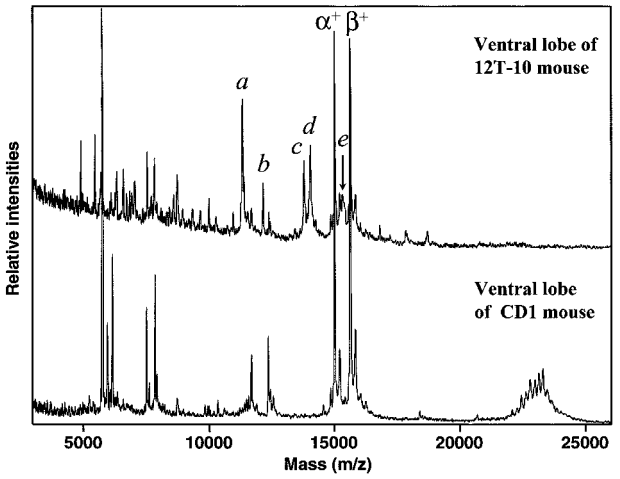

Figure 9. MALDI MS protein profiles obtained from the ventral lobe of 12T-10 transgenic mouse and non-transgenic control mouse. Five distinct groups of signals (labeled **a** to **e**) were specifically observed in the ventral lobe of the 12T-10 mouse. Other signals such as the ones between *m/z* 22,000 and 24,000 were found specific to the ventral lobe of non-transgenic CD1 mouse. The α+ and β+ symbols indicate the α- and β-chain of hemoglobin, respectively.

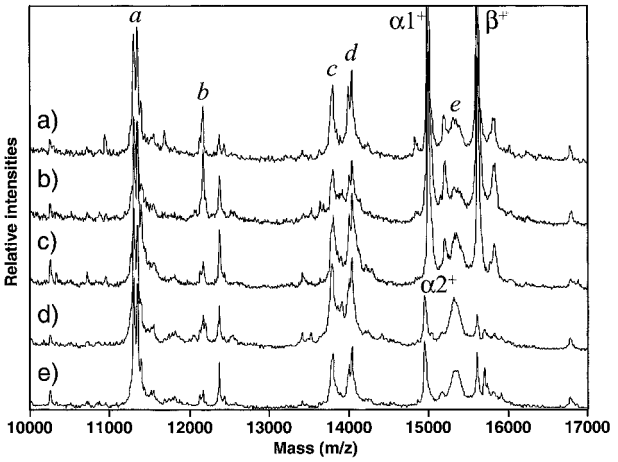

Figure 10. MALDI MS protein profiles obtained from the ventral lobe (**a**), lymph node (**b**), and liver nodule (**c**) of 12T-10 transgenic mouse; and from a subcutaneously inoculated NE tumor **d**) and and liver metastasis (**e**) in an athymic nude mouse. All of the profiles showed very similar protein profiles in particular the five groups of signals from **a** to **e.** The α+ and β+ symbols indicate the α- and β-chain of hemoglobin, respectively. Note that the molecular weight of the α-chain was found different between the two strains of mice (labeled α1 and α2).

microscopy). The photomicrographs show a number of astrocytes in the high-grade tumor with pronounced S100β immunoreactivity in the cytosol (arrowhead) and weak immunopositivity in the oligodendrocytes in the low-grade tumor. Similar IMS and immunostaining patterns have been seen when comparing grade IV astrocytomas with grade II astrocytomas.

Monitoring Cancer Progression

Profiling MALDI mass spectrometry has been used to monitor alterations in protein expression associated with tumor progression and metastasis in a mouse model. The 12T-10 transgenic mouse[43] expressing the rat prostate-specific large probasin (LPB) promoter linked to the SV40-large T antigen (Tag) which develops prostatic neoplasia has been recently characterized.[44] This is a transgenic model of prostate adenocarcinoma (PCA) with progressive neuroendocrine (NE) differentiation. Mass spectrometric analyses were performed using a tissue-blotting approach[45] on a polyethylene membrane.[46] Analysis of a poorly or undifferentiated carcinoma from the ventral lobe of a 38-week-old 12T-10 mouse showed distinct and specific protein profiles compared to the ventral lobe of a non-transgenic CD1 mouse (Figure 9). For example, the signals observed in the *m/z* range from 22,000 to 24,000 were found to be unique to the ventral lobe of the non-transgenic CD1 mouse. These signals have been found to correspond to a glycoprotein identified as the spermine-binding protein.[47] Numerous signals were found uniquely expressed in the PCA from the 12T-10 ventral prostate lobe. In particular, five distinct groups of signals (Figure 10, labeled a to e) in the *m/z* range from 10,000 to 17,000 were observed that were not detected in the ventral lobe of the non-transgenic CD1 mouse. Signal a contained at least five different ions at *m/z* 11,265, 11,307, 11,349, 11,391, and 11,433. The signal distribution was Gaussian-shaped, suggesting multiple random acetylations. These signals have been found to correspond to multiply acetylated forms of the histone H4. Signal b displayed two major peaks at *m/z* 12,134 and 12,167. The signal observed at *m/z* 12,134 was subsequently identified as cytochrome C. Signal *c* displayed two major peaks at *m/z* 13,777 and 13,804. The signal observed at 13,804 Da was identified as the histone H2B1. Signal d contained three distinct mass peaks at *m/z* 14,005, 14,047, and 14,089. These correspond to the histone H2A.2 and its diacetylated forms and to the histone H2A.1, respectively. Signal e was located between the α- and the β-chains of hemoglobin. This signal centered on *m/z* 15,355 was broad and unresolved, indicating the presence of several different proteins or protein isoforms within a close mass range. This broad signal was identified as the multiple isoforms of the histone H3.

The 12T-10 mice studied also displayed several enlarged lymph nodes and the presence of liver nodules. On analysis, these regional lymph nodes and nodules showed very similar protein profiles as the ventral lobe tumor including the a through e signals (Figure 10, a to c). Furthermore, these secondary tumors showed histological features of NE differentiation, which were confirmed by chromogranin immunohistochemical staining and electron microscopy, suggesting prostatic origin. To further assess the metastatic potential of the undifferentiated carcinoma developing in the 12T-10 prostate, portions of the grossly abnormal ventral lobe of a 38-week-old 12T-10 mouse, which had histologically confirmed undifferentiated carcinoma, were transplanted subcutaneously into an athymic male mouse. A histologically identical NE carcinoma grew at the primary transplant site and the mouse developed Tag-positive, histologically identical metastases in the liver (confirmed histologically at 18 weeks post-transplant). NE differentiation was confirmed by chromogranin A immu-

nohistochemistry and electron microscopy. MALDI MS protein profiles of the subcutaneously inoculated NE carcinoma from the athymic nude mouse and its liver metastasis also showed the same protein profiles as those seen in the NE carcinoma containing the ventral lobe of the 12T-10 transgenic line (Figure 10). These findings, in association with histology and/or Tag immunohistochemistry, further supported that lesions in the extraprostatic organs were metastases from the prostate.

In this study, primary and metastatic undifferentiated/NE tumors had essentially identical profiles, which were also distinct compared to wild-type prostate. Histones, typically nuclear proteins, were observed in NE carcinoma in high abundance by mass spectrometry. This may be related to high nuclear to cytoplasmic ratios of NE cancer cells. When the tissue sections were prepared, inevitably a non-negligible percentage of the cell nuclei were ruptured and their protein content was accessible to the blotting membrane. Although histones themselves are not specific for NE cancer, detection of large amounts of histones may be a marker of proliferation in NE cancer cells because only 12T-10 prostates and those metastases containing NE cancer cells showed the clusters of signals a through e. The unidentified signals at *m/z* 12,167 in the b cluster and at *m/z* 13,777 in the c cluster as well as numerous others, may be NE cancer-specific markers of the 12T-10. Thus, mass spectrometric analysis of tissue sections may become one strategy to characterize the changes in protein expression profiles during tumor progression as well as to help establish sites of primary origin for metastatic tumors.

Perspectives and Future Applications

Imaging mass spectrometry is a new technology that is currently undergoing further development to make it more routinely accessible to users. Imaging time depends on several instrumental parameters, namely the laser repetition rate, spot-to-spot sample repositioning, and data processing. Lasers with repetition rates at or above one kilohertz and improved electronics will considerably reduce acquisition times from hours to minutes. Acquisition algorithms capable of recording high-throughput data and specially targeted data mining tools are also being developed. Imaging resolution, currently in the 50-μm range for tissue level analysis, may be increased to 1 to 5 μm for applications requiring subcellular analyses. Such developments are ongoing.[39] Efforts to improve sample preparation and matrix-coating procedures are also being undertaken to provide protocols that more easily achieve high sensitivity and high resolution images.[40,41] The potential of such a molecular imaging technology is considerable. The fundamental contributions of the technology in rapidly providing molecular weight specific images will provide important information in the investigation of cellular processes in both health and disease.

The enormous potential of a highly sensitive and molecularly specific technology such as mass spectrometry to the fields of medicine and biology are just being realized. From work already published, it is clear that the integration of this technology into protocols for disease diagnosis as well as outcome prediction will soon take place. As protein expression data becomes available from various tissue types, this approach will provide a common disease-wide approach that can be applied to many specific problems. For example, one can envision the use of MS technology to evaluate a "tumor of unknown primary." Current data suggests that MALDI MS will be highly superior to immunohistochemical stains and electron microscopy in identifying the site of origin for such tumors. Given significant differences in therapy, the "tumor of unknown primary" is a critical dilemma in oncology practice.

One can also foresee the use of this MS technology in several current problems in diagnostic pathology. For example, some tumor types are notorious for requiring several tissue samplings to obtain adequate tissue to establish a diagnosis despite high clinical suspicion. Few oncologists would proceed with treatment without an established tissue diagnosis. Two such examples are mesothelioma and small cell lung cancer (SCLC). With respect to mesothelioma, besides acquiring adequate tissue for diagnosis, the additional dilemma of its distinction from a metastasis, pulmonary adenocarcinoma, or even a reactive mesothelial process can be challenging. Immunohistochemistry and electron microscopy are currently the ancillary techniques used. Diagnostic challenges related to SCLC and its distinction from other neuroendocrine tumors of the lung requiring less aggressive therapy are many. The full spectrum of neuroendocrine carcinomas would be expected to show varying degrees of "crush artifact" on transbronchial biopsy. Unless sufficient tumor can be visualized on a slide such that a mitotic count can be performed and nuclear atypia assessed, distinction of a large cell neuroendocrine carcinoma from small cell or even an atypical carcinoid can be particularly problematic. Immunohistochemical stains are not particularly useful in this regard as they would all stain positive and in all cases neuroendocrine granules would be present on electron microscopy. As demonstrated by the lung tumor proteomic studies,[19] this distinction, as well as some prognostic predictions, could be made rapidly with MALDI MS.

Another application of MALDI MS in surgical pathology would be the rapid evaluation of surgical margins. There are several examples where analysis of surgical margins by frozen section is very difficult if not impossible, including lobular breast cancer, signet ring carcinomas of the gastrointestinal tract, and cholangiocarcinoma. Each of these cancers is well known to invade in a single cell fashion and without producing a grossly identifiable mass. Given the sensitivity of MS, we envision that even a few tumor cells could be detected within a significantly larger portion of tissue. The practical implementation of MS for intra-operative margin assessment is likely to require a significant reduction in data acquisition and analysis time for scanning MS techniques to be useful in this regard. In addition, reliable and generalizable markers of

neoplasia would facilitate this analysis and await proteomic analysis of large numbers of various neoplasms.

The potential capability of MALDI MS to measure susceptibility and response to therapeutic agents in tumor and surrounding tissues is a particularly exciting application of this technology. First, the original protein profile obtained from the primary tumor could be used to influence the selection of therapeutic agents. Levels of drugs such as chemotherapeutic agents or hormonal therapies such as Herceptin or Tamoxifen, etc could be measured directly from a tissue biopsy to assess adequacy of delivery to a particular organ site. The ability of drugs and other bioreactive molecules to adequately penetrate larger tumors has long been known to be problematic and could be more adequately assessed by this technology. In addition, alterations in specific molecular pathways directly modulated or indirectly affected by the agent could be evaluated. This analysis could be sequential beginning within minutes of initiating therapy and then continued at regular intervals. Studies of this type that clearly establish proof of principle have been reported.[23] Similar methods could be envisioned to monitor patients treated with conservative therapy for relapse.

Finally, one must take note that the MS technology described in this article for profiling and imaging of tissue biopsies is newly developed and the instrumentation used has not yet been fully optimized and specifically tailored to this field. One can expect significant advances in the sensitivity, speed, and biocomputational aspects of this technology will be directly focused on the application of diagnostic pathology. Molecular discovery in disease processes and its integration in diagnostic pathology is already underway and new technologies, such as mass spectrometry, provide an ideal vehicle into this arena. Proteomics of disease will likely play a major role in pathology in the years to come, allowing us to assess disease presence and progression, predict patient outcomes, predict the efficacy of therapies, and provide for very early detection of disease. Together with genomics and perhaps additional molecular information describing the state of lipids and metabolites, proteomics provides an entry into individualized medicine, where each patient's disease is unique at the molecular level and will be treated in such manner.

Acknowledgments

We thank Axel Ducret (Ph.D.) and Hélène Meistermann (F. Hoffmann-La Roche Ltd, Bazel, Switzerland) for their contributions to Figure 5, Jonathan Xu (Mass Spectrometry Research Center, Vanderbilt University) for his help in generating the data presented in Figure 6, Malin Andersson (Ph.D.) and Sarah Schwartz (Ph.D., Mass Spectrometry Research Center, Vanderbilt University) for their contributions to Figure 8. We especially thank Hans-Rudolf Aerni (Mass Spectrometry Research Center, Vanderbilt University) for his valuable help in generating the mass spectrometry data presented in Figures 5 and 8. Finally, we thank MDS Inc. (Odense, Denmark) for the S100β protein identification and John Floyd (M.D., Department of Neurosurgery, Vanderbilt University) for his useful comments and critical reading of the manuscript.

References

1. Roepstorff P: Mass spectrometry in protein studies from genome to function. Curr Opin Biotechnol 1997, 8:6–13
2. Russell DH, Edmondson RD: High-resolution mass spectrometry and accurate mass measurements with emphasis on the characterization of peptides and proteins by matrix-assisted laser desorption/ionization time-of-flight mass spectrometry. J Mass Spectrom 1997, 32: 263–276
3. Lahm HW, Langen H: Mass spectrometry: a tool for the identification of proteins separated by gels. Electrophoresis 2000, 21:2105–2114
4. Pandey A, Mann M: Proteomics to study genes and genomes. Nature 2000, 405:837–846
5. McDonald WH, Yates JR: Proteomic tools for cell biology. Traffic 2000, 1:747–754
6. Aebersold R, Goodlett DR: Mass spectrometry in proteomics. Chem Rev 2001, 101:269–295
7. Godovac-Zimmermann J, Brown LR: Perspectives for mass spectrometry and functional proteomics. Mass Spectrom Rev 2001, 20: 1–57
8. Karas M, Hillenkamp F: Laser desorption ionization of proteins with molecular masses exceeding 10,000 daltons. Anal Chem 1988, 60: 2299–2301
9. Hillenkamp F, Karas M, Beavis RC, Chait BT: Matrix-assisted laser desorption ionization mass-spectrometry of biopolymers. Anal Chem 1991, 63:1193A–1202A
10. Brown RS, Lennon JJ: Mass resolution improvement by incorporation of pulsed ion extraction in a matrix-assisted laser-desorption ionization linear time-of-flight mass-spectrometer. Anal Chem 1995, 67: 1998–2003
11. Vestal ML, Juhasz P, Martin SA: Delayed extraction matrix-assisted laser-desorption time-of-flight mass-spectrometry. Rapid Commun Mass Spectrom 1995, 9:1044–1050
12. Stoeckli M, Chaurand P, Hallahan DE, Caprioli RM: Imaging mass spectrometry: a new technology for the analysis of protein expression in mammalian tissues. Nat Med 2001, 7:493–496
13. Todd PJ, Schhaaff TG, Chaurand P, Caprioli RM: Organic ion imaging of biological tissue with SIMS and MALDI. J Mass Spectrom 2001, 36:355–369
14. Chaurand P, Caprioli RM: Direct profiling and imaging of peptides and proteins from mammalian cells and tissue sections by mass spectrometry. Electrophoresis 2002, 23:3125–3135
15. Chaurand P, Schwartz SA, Caprioli RM: Imaging mass spectrometry: a new tool to investigate the spatial organization of peptides and proteins in mammalian tissue sections. Curr Opin Chem Biol 2002, 6:676–681
16. Stoeckli M, Staab D, Staufenbiel M, Wiederhold K-H, Signor L: Molecular imaging of amyloid beta peptides in mouse brain sections using mass spectrometry. Anal Biochem 2002, 311:33–39
17. Chaurand P, Fouchecourt S, DaGue BB, Xu BJ, Reyzer ML, Orgebin-Crist MC, Caprioli RM: Profiling and imaging proteins in the mouse epididymis by imaging mass spectrometry. Proteomics 2003, 3:2221–2239
18. Chaurand P, Schwartz SA, Caprioli RM: Profiling and imaging proteins in tissue sections by mass spectrometry. Anal Chem 2004, 76:86A–93A
19. Yanagisawa K, Shyr Y, Xu BJ, Massion PP, Larsen PH, White BC, Roberts JR, Edgerton M, Gonzalez A, Nadaf S, Moore JH, Caprioli RM, Carbone DP: Proteomic patterns of tumor subsets in non-small-cell lung cancer. Lancet 2003, 362:433–439
20. Schwartz SA, Weil RJ, Johnson MD, Toms SA, Caprioli RM: Protein profiling in brain tumors using mass spectrometry: feasibility of a new technique for the analysis of protein expression. Clin Cancer Res 2004, 10:981–987
21. Chaurand P, Schwartz SA, Caprioli RM: Assessing protein patterns in disease using imaging mass spectrometry. J Proteome Res 2004, 3:245–252
22. Troendle FJ, Reddick CD, Yost RA: Detection of pharmaceutical compounds in tissue by matrix-assisted laser desorption/ionization

and laser desorption/chemical ionization tandem mass spectrometry with a quadrupole ion trap. J Am Soc Mass Spectrom 1999, 10:1315–1321
23. Reyzer ML, Hsieh Y, Ng K, Korfmacher WA, Caprioli RM: Direct analysis of drug candidates in tissue by matrix-assisted laser desorption/ionization mass spectrometry. J Mass Spectrom 2003, 38:1081–1092
24. EmmertBuck MR, Bonner RF, Smith PD, Chuaqui RF, Zhuang ZP, Goldstein SR, Weiss RA, Liotta LA: Laser capture microdissection. Science 1996, 274:998–1001
25. Bonner RF, EmmertBuck M, Cole K, Pohida T, Chuaqui R, Goldstein S, Liotta LA: Cell sampling: laser capture microdissection: molecular analysis of tissue. Science 1997, 278:1481–1483
26. Bichsel VE, Petricoin EF, Liotta LA: The state of the art microdissection and its downstream applications. J Mol Med 2000, 78:B20–B20
27. Palmer-Toy DE, Sarracino DA, Sgroi D, LeVangie R, Leopold PE: Direct acquisition of matrix-assisted laser desorption/ionization time-of-flight mass spectra from laser capture microdissected tissues. Clin Chem 2000, 46:1513–1516
28. Xu BJ, Caprioli RM, Sanders ME, Jensen RA: Direct analysis of laser capture microdissected cells by MALDI mass spectrometry. J Am Soc Mass Spectrom 2002, 13:1292–1297
29. Bhattacharya SH, Gal AA, Murray KK: Laser capture microdissection MALDI for direct analysis of archival tissue. J Proteome Res 2003, 2:95–98
30. Stoeckli M, Farmer TB, Caprioli RM: Automated mass spectrometry imaging with a matrix-assisted laser desorption ionization time-of-flight instrument. J Am Soc Mass Spectrom 1999, 10:67–71
31. Schwartz SA, Reyzer ML, Caprioli RM: Direct tissue analysis using matrix-assisted laser desorption/ionization mass spectrometry: practical aspects of sample preparation. J Mass Spectrom 2003, 38:699–708
32. Kruse R, Sweedler JV: Spatial profiling invertebrate ganglia using MALDI MS. J Am Soc Mass Spectrom 2003, 14:752–759
33. Fournier I, Day R, Salzet M: Direct analysis of neuropeptides by in situ MALDI-TOF mass spectrometry in the rat brain. Neuroendocrinol Lett 2003, 24:9–14
34. Bahr U, StahlZeng J, Gleitsmann E, Karas M: Delayed extraction time-of-flight MALDI mass spectrometry of proteins above 25,000 Da. J Mass Spectrom 1997, 32:1111–1116
35. Brunelle A, Chaurand P, DellaNegra S, LeBeyec Y, Parilis E: Secondary electron emission yields from a CsI surface under impacts of large molecules at low velocities ($5 \times 10(3) - 7 \times 10(4)$ ms(-1)). Rapid Commun Mass Spectrom 1997, 11:353–362
36. Westmacott G, Frank M, Labov SE, Benner WH: Using a superconducting tunnel junction detector to measure the secondary electron emission efficiency for a microchannel plate detector bombarded by large molecular ions. Rapid Commun Mass Spectrom 2000, 14:1854–1861
37. Chaurand P, Schwartz SA, Billheimer D, Xu BJ, Crecelius A, Caprioli RM: Integrating histology and imaging mass spectrometry. Anal Chem 2004, 76:1145–1155
38. Garden RW, Sweedler JV: Heterogeneity within MALDI samples as revealed by mass spectrometric imaging. Anal Chem 2000, 72:30–36
39. Spengler B, Hubert M: Scanning microprobe matrix-assisted laser desorption ionization (SMALDI) mass spectrometry: instrumentation for sub-micrometer resolved LDI and MALDI surface analysis. J Am Soc Mass Spectrom 2002, 13:735–748
40. Aerni HR, Erskine AR, Reyzer ML, Lee D, Cornett DS, Caprioli RM: Unique robotic matrix spotter for MALDI imaging. Proceedings of the 51st ASMS Conference on Mass Spectrometry and Allied Topics, Montreal, Quebec, Canada, 2003
41. Aerni HR, Cornett DS, Chaurand P, Suzuki K, Orgebin-Crist MC, Daikoku T, Dey SK, Caprioli RM: Automated sample preparation for MALDI imaging MS. Proceedings of the 52nd ASMS Conference on Mass Spectrometry and Allied Topics, Nashville TN, 2004
42. Chaurand P, DaGue BB, Pearsall RS, Threadgill DW, Caprioli RM: Profiling proteins from azoxymethane-induced colon tumors at the molecular level by matrix-assisted laser desorption/ionization mass spectrometry. Proteomics 2001, 1:1320–1326
43. Kasper S, Sheppard PC, Yan YL, Pettigrew N, Borowsky AD, Prins GS, Dodd JG, Duckworth ML, Matusik RJ: Development, progression, and androgen-dependence of prostate tumors in probasin large T antigen transgenic mice: a model for prostate cancer. Lab Invest 1998, 78:319–333
44. Masumori N, Thomas TZ, Chaurand P, Case T, Paul M, Kasper S, Caprioli RM, Tsukamoto T, Shappell SB, Matusik RJ: A probasin-large T antigen transgenic mouse line develops prostate adenocarcinoma and neuroendocrine carcinoma with metastatic potential. Cancer Res 2001, 61:2239–2249
45. Caprioli RM, Farmer TB, Gile J: Molecular imaging of biological samples: localization of peptides and proteins using MALDI-TOF MS. Anal Chem 1997, 69:4751–4760
46. Chaurand P, Stoeckli M, Caprioli RM: Direct profiling of proteins in biological tissue sections by MALDI mass spectrometry. Anal Chem 1999, 71:5263–5270
47. Chaurand P, DaGue BB, Ma SG, Kasper S, Caprioli RM: Strain-based sequence variations and structure analysis of murine prostate-specific spermine-binding protein using mass spectrometry. Biochemistry 2001, 40:9725–9733